Ehrlich-Schwoebel instability in molecular-beam epitaxy: A minimal model

Paolo Politi and Jacques Villain
CEA, Département de Recherche Fondamentale sur la Matière Condensée, Service de Physique des Matériaux & Microstructures/ Nanostructures et Magnétisme, 38054 Grenoble Cedex 9, France
and CEA, Département de Recherche Fondamentale sur la Matière Condensée, Service de Physique Statistique, Magnétisme, et Supraconductivité, 38054 Grenoble Cedex 9, France
(Received 20 February 1996)

The instability of a growing crystal limited by a high-symmetry surface in molecular-beam epitaxy is studied in the limit where terrace size is very large compared to the atomic distance. In that case, everything is deterministic except the nucleation of new terraces. Moreover, exchange of atoms between steps is ignored. If the typical terrace size ℓ_c is chosen as length unit, the model depends on a single parameter (ℓ_s/ℓ_c) which characterizes the strength of step-edge barriers (''Ehrlich-Schwoebel effect''). Numerical simulations are supported by nonlocal evolution equations relating the time and space derivatives of the surface height. The first mounds which appear have a radius $\lambda_c^{\rm inf}$ proportional to $\ell_c\sqrt{\ell_c/\ell_s}$. In contrast with other authors who studied different models, coarsening is found to become extremely slow after the mounds have reached a radius $\lambda_c^{\rm sup}$ of order ℓ_c^2/ℓ_s. [S0163-1829(96)10631-7]

I. THE EHRLICH-SCHWOEBEL INSTABILITY

This article is devoted to a well-known instability[1,2] which occurs in molecular-beam epitaxy at low temperature: if the growing crystal is limited by a surface of high-symmetry orientation, the growth generates the formation of ''terraces'' of atomic height.[3,4] In the presence of an extra energy barrier[1] which hinders interlayer diffusion, atoms landing on these terraces cannot easily step down[1,2] and therefore nucleate new terraces. Since grooves are not easily filled up, eventually towers or ''mounds'' form. Such mounds have been observed experimentally on a variety of systems: Si,[5] Ge,[6] GaAs,[7,8] Cu,[9] and Fe.[10–12]

So far, the most complete theoretical studies have been numerical.[8,13–18] They confirm the existence of mounds, whose size increases with time due to coalescence. However, the laws of this *coarsening* are, neither experimentally nor theoretically clear: in certain cases the mound shapes remain self-similar during coarsening[7,9,11,12,16,17] while in other cases they become sharper.[6,10,16,18] Also, the impossibility to study very long times, accompanied by a slop steepening, may sometimes prevent from drawing firm conclusions.

The purpose of the present work is to clarify the coarsening mechanism in 1+1 dimensions (one-dimensional surface in a two-dimensional space). We hope that this study may give information about the physical, (2+1)-dimensional growth problem.

In the following it will be useful to distinguish ''top'' terraces, ''bottom'' terraces, and ''vicinal'' terraces, i.e., those which have both a lower edge and an upper edge (Fig. 1). Let $z(\vec{r},t)$ be the height of the surface above its average position $h(t)=aFt$. Both z and h are measured in atomic layers. If evaporation is neglected, z satisfies the conservation equation

$$\frac{\partial z}{\partial t} = -a^{d'}\vec{\nabla}\cdot\vec{j}(\vec{r},t)+\delta f(\vec{r},t), \tag{1.1}$$

where $d'=d-1$ is the surface dimension (1 in this paper, 2 in reality), and the random function $\delta f(\vec{r},t)$ is the fluctuation of the atomic beam (called shot noise in jargon). The current $\vec{j}$ is measured in particles per unit time (in $d=1+1$ dimensions) or in particles per unit time and unit length (in $d=2+1$ dimensions). It is generally written as the following phenomenological equation:[3,8,15,19]

$$\vec{j}(\vec{r},t)=\vec{\psi}(\vec{\nabla}z(\vec{r},t))+K\vec{\nabla}(\nabla^2 z(\vec{r},t))+\vec{f}_j(\vec{r},t). \tag{1.2}$$

Here, the random function $\vec{f}_j(\vec{r},t)$ corresponds to the fluctuation of the adatom current around its expected average value given by the diffusion equation. The phenomenological constant K is generally traced back to the exchange of atoms between terraces, which results from thermal fluctuations and tends to smooth the surface. We shall come back to this point later, and suggest another possible origin.

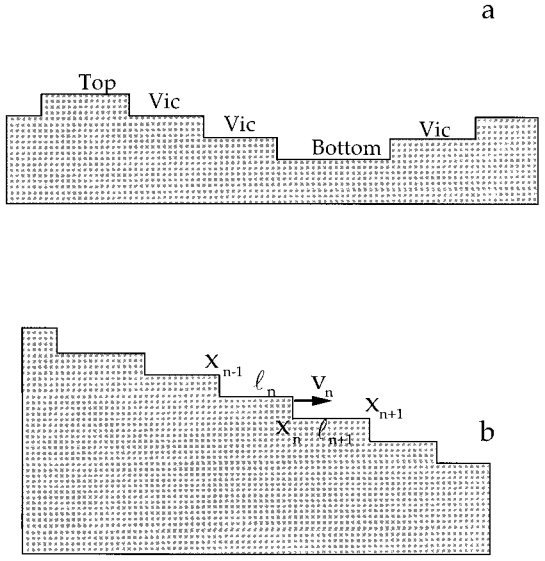

FIG. 1. Typical profile of a (1+1)-dimensional growing crystal. (a) Top terraces (*top*), vicinal terraces (*vic*), and bottom terraces (*bottom*). (b) In the Zeno model, the velocity v_n of a step is a function of the widths ℓ_n and ℓ_{n+1} of the neighboring terraces.

The nature of the function $\psi(\vec{\nabla}z(\vec{r},t))$ is, of course, essential. Since the current $\vec{\psi}$ must vanish on the high-symmetry orientation, for small fluctuations of $\vec{\nabla}z$ around its equilibrium value 0, one can assume[3,8,15]

$$\psi(\vec{\nabla}z)=B\vec{\nabla}z. \tag{1.3}$$

As a consequence of the Ehrlich-Schwoebel effect, adatoms on a vicinal terrace preferably stick to the upper edge and this means that the average current should have the same direction and sense as ∇z. So the coefficient B is positive and the first term of (1.2) formally reduces Eq. (1.1) to a diffusion equation, but with a negative diffusion constant $-B$. It follows that the spatial Fourier transform $z_k(t)$ of $z(\vec{r},t)$ diverges: $z_k(t)=z_k(0)\exp(Bk^2t)$. This is the manifestation of the Zeno-Schwoebel instability: a plane surface is unstable, even if—as seen below—the second term in (1.2) stabilizes against short wavelength fluctuations. However, the evolution can be precise only if a more complicated form is used for the function $\psi(\vec{\nabla}z)$. Johnson *et al.*[8] have interpolated between (1.3), valid at small slopes, and the expression $\psi(\vec{m})\sim 1/m$ (with $\vec{m}\equiv\vec{\nabla}m$), which was expected to be correct at high slopes, obtaining the form

$$\psi(\vec{m})=B\frac{\vec{m}}{1+\ell_d^2m^2}, \tag{1.4}$$

where ℓ_d is a length. Since $\psi(\vec{m})$ has always the same sign as $\vec{m}$, all the directions are unstable and deeper and deeper grooves are expected to form.

Siegert and Plischke[15] have suggested that, due to the details of the crystal structure, the function $\psi(\vec{m})$ should become negative beyond some characteristic value m^* of the slope. So $\partial\psi/\partial m|_{m^*}<0$ and the slope m^* would be stable against small fluctuations of the orientation.

For instance, if the crystal is face centered cubic and the average surface is (001), it is conceivable that the local slope cannot go beyond that of a (111) orientation, since otherwise overhangs would form. Such a suggestion turned out to be correct in the case of heteroepitaxial growth of Fe/MgO (Ref. 11) and it is in agreement with the findings of Ernst *et al.*[9] on Cu/Cu.

The slope selection has been recently discussed also by Šmilauer and Vvedensky[16] and by Amar and Family,[17] who perform simulations on solid-on-solid models. The first ones introduce a transient mobility just after the adatom has dropped on the surface, while Amar and Family consider a downward funneling, determined by the search of a fourfold hollow site. The resulting final slopes are appreciably smaller than those obtained by Siegert and Plischke.

In the present work, the fluctuating functions $\delta f(\vec{r},t)$ and $\vec{f}_j(\vec{r},t)$ will be assumed negligible. This is correct when all terrace sizes are much larger than the atomic distance a because, in that case, many atoms are necessary to produce a given displacement of the steps, and the relative fluctuation of the number of atoms is negligible. The case of $\delta f(\vec{r},t)$ is discussed in detail in Ref. 3.

Thus, we want to investigate a model in which the only source of stochasticity is the nucleation of new terraces, which does not become deterministic in the limit of small a. In addition, we mainly address the case when atoms cannot detach from steps and be exchanged between terraces. This situation is, in practice, realized at low temperature.[20] In this case, we shall argue that (i) Eq. (1.2) has to be modified, but a straightforward modification does account for the onset of the instability. Also, the term in K will be shown to be present even in absence of thermal detachment. (ii) The evolution of the patterns which appear at longer times can only be accounted for by a nonlocal modification of (1.2). (iii) Only at very long times large slopes appear.

II. BASIC EQUATIONS AND PARAMETERS OF THE MODEL

In a growth problem, there are generally many parameters. The model we shall study, initially proposed by Elkinani and Villain,[18] has the advantage to contain only two characteristic lengths, which may be called nucleation length and Schwoebel length. Only the ratio of these lengths has a nontrivial effect on the properties of the system, which therefore depends on a single significant parameter.

The nucleation length ℓ_c is qualitatively defined as the typical width of a terrace just before a new terrace is nucleated at the top of it. The Schwoebel length ℓ_s is defined as follows: if the width ℓ of a ''vicinal'' terrace is smaller than ℓ_s, most of the atoms landing on this terrace go to its upper edge, while if $\ell\gg\ell_s$, about one-half of the atoms go to each edge because they are too far from the other one.

In the simplest approximation, the atomic distance a is just assumed to be infinitely small. This *continuous Zeno model* can only be good in the continuum limit $a\ll\ell_s,\ell_c$. Moreover, we are mainly interested by the case $\ell_s\ll\ell_c$, because in the opposite case, deep crevaces appear very early,[18,21] and no good crystal can be grown. Thus, we focus our interest on the case

$$a\ll\ell_s\ll\ell_c. \tag{2.1}$$

Even if (2.1) holds, terraces of width $\ell\approx a$ appear at very long times. The behavior at these long times depends on the microscopic features of the system and, as will be seen in Sec. XIV. These long times are not necessarily of practical interest, if the purpose is just to obtain a smooth surface and if one does not care about what happens after the onset of the instability. In the forthcoming sections, a will be assumed infinitely small.

In the simulations it is not easy to fulfill condition (2.1), because it would require terraces of several tens of lattice constants. Anyway, it is not a bad approximation, as can be seen from Refs. 8,16 and 17. In Johnson *et al.*[8] $\ell_s/a\simeq 1$–10 and $\ell_s/\ell_c\simeq 0.04$–0.8. In Refs. 16 and 17 ℓ_c can be estimated as a measure of the average terrace size and ℓ_s can be deduced from the minimal mound size, as given by formula (3.6) below. It results that $\ell_c/a\simeq 10$–20 and $\ell_s/\ell_c\simeq 0.1$–1. Thus, condition (2.1) is a reasonable assumption.

We shall generally consider a $(1+1)$-dimensional model in which[18]

$$\ell_s=a\left(\frac{D}{D'}-1\right) \tag{2.2}$$

and

$$\ell_c^3(\ell_c+6\ell_s)=\frac{12Da}{F}, \tag{2.3}$$

where F is the beam intensity in atoms per unit time and unit length, D is the diffusion constant, and D'/a^2 is the hopping rate for an atom wanting to step down.

The evolution of the surface is determined by the local step velocity, which is the sum of two terms, proportional to the local gradient of the adatom density $\rho(\vec{r})$ on both sides of each step. The adatom density is in turn determined by the diffusion equation[22]

$$\dot{\rho}(\vec{r},t)=F+D\nabla^2\rho(\vec{r},t) \tag{2.4}$$

and by appropriate boundary conditions on steps.[4,23] In (2.4), the fluctuating functions $\delta f(\vec{r},t)$ and $\vec{f}_j(\vec{r},t)$ have been assumed negligible, as justified in Sec. I.

In 1+1 dimensions it is easy to eliminate the adatom density $\rho(\vec{r},t)$ (Ref. 18) and the velocity of a step is found to be (see Fig. 1)

$$v_n=f(\ell_n)+g(\ell_{n+1}), \tag{2.5}$$

where ℓ_n and ℓ_{n+1} are, respectively, the width of the upper and lower terraces, and the functions $f(\ell)$ and $g(\ell)$ have different definitions for top, bottom, and vicinal terraces. For vicinal terraces,

$$f(\ell)=\frac{aF\ell}{2}\left(1-\frac{\ell_s}{\ell+\ell_s}\right) \tag{2.6}$$

and

$$g(\ell)=\frac{aF\ell}{2}\left(1+\frac{\ell_s}{\ell+\ell_s}\right). \tag{2.7}$$

For top terraces,

$$f(\ell)=\frac{aF\ell}{2} \tag{2.8}$$

and for bottom terraces

$$g(\ell)=\frac{aF\ell}{2}. \tag{2.9}$$

In addition, new terraces are created on a terrace of width ℓ with a probability $P_{\rm nucl}(\ell)$ per unit time, which increases abruptly as soon as ℓ becomes of order ℓ_c. Elkinani and Villain[18] used the formula

$$P_{\rm nucl}(\ell)=\frac{F^2\ell^4}{12D}\left(1+\frac{6\ell_s}{\ell}\right). \tag{2.10}$$

These equations should be complemented by an equation for the probability of the location of the newly nucleated terraces, which can be deduced from the Burton-Cabrera-Frank theory associated with a model for terrace nucleation.[23–26] The details will not be recalled here.

A deterministic version of nucleation process, which will be occasionally used in the present work, is also possible; in this case a new terrace nucleates on an old one, at the place where the adatom density $\rho(x)$ is maximum, when the width of this terrace becomes equal to the value ℓ_c defined by (2.3). This condition can be obtained by writing that the probability of nucleation on a terrace of width ℓ_c during the deposition of one layer, is of order 1.

For a vanishing Schwoebel effect ($\ell_s=0$), (2.10) reads

$$P_{\rm nucl}(\ell)=aF\left(\frac{\ell}{\ell_c}\right)^4. \tag{2.11}$$

If the time unit is chosen as $1/(Fa)$, the filling time of a layer, and if the length unit is chosen as ℓ_c, the ''Zeno equations'' (2.5)–(2.10) become parameter free, and, in particular, independent of a. It is easily seen that the spatial distribution of the nucleation probability at a given time is also parameter free. Therefore, all properties of the model for $\ell_s=0$ depend only on Fat and ℓ/ℓ_c. For instance,

$$\frac{\partial z}{\partial(Fat)}=\Phi(\ell_c m,\ell_c^2\partial_x m,\dots), \tag{2.12}$$

where $\Phi(u,v,\dots)$ is a function.

The Zeno equations (2.5)–(2.10) allow for a numerical solution of the problem. However, they do not provide much insight because they give information on objects (steps) which are perpetually created and annihilated, and whose number perpetually changes in a way which is not easy to predict from these equations. In the rest of this paper, we shall try to derive more explicit information from the Zeno equations. The system is generally assumed to be 1+1 dimensional, but conjectures about the (2+1)-dimensional case will be presented in Sec. XV.

III. ONSET OF THE INSTABILITY

In Sec. I, we related the surface evolution to the current density. In the case of an uniform absolute slope $|m|=1/\ell$, the average current density

$$j(\ell)=\frac{1}{\ell}\int_{-\ell/2}^{\ell/2}j(x)dx$$

can be obtained using the expression

$$j(x)=Fx+\frac{j(\ell/2)+j(-\ell/2)}{2},$$

which results from integrating (2.4) if the left-hand side is neglected. Since $j(\ell/2)=f(\ell)/a$ and $j(-\ell/2)=-g(\ell)/a$, the result, for negative slopes (see Fig. 1) is

$$j(\ell)=\frac{f(\ell)-g(\ell)}{2a}=-\frac{F\ell\ell_s}{2(\ell+\ell_s)}=-\frac{F\ell_s}{2(1+|m|\ell_s)}. \tag{3.1}$$

We have used Eqs. (2.6) and (2.7) which are only valid on vicinal terraces, so that (3.1) is not valid if $|m|\ell_c<1$. As seen in Sec. I, the current density is expected to be proportional to m for small values of $m=\partial z/\partial x$ (see also Appendix B). A reasonable interpolation is therefore

$$j=\frac{F\ell_s\ell_c m}{2(1+|m|\ell_s)(1+|m|\ell_c)}. \tag{3.2}$$

A more precise expression, containing also higher order derivatives of $z(x)$, will be derived in Sec. VI. Expression (3.2) is analogous, but not identical to Eq. (1.4) proposed by Johnson *et al.*,[8] which contains a single length instead of the two lengths ℓ_s and ℓ_c. This forbids us, by rescaling the current and/or the slope $|m|$, to put the above expression for j in an ''universal'' form, which does not depend on ℓ_s and ℓ_c. Such a rescaling is possible for the current proposed by Johnson *et al.*,[8] because they start by supposing an infinite Schwoebel effect. In this case only the length ℓ_c appears and it is reasonable to think that a universal function can be obtained. Then, if the Schwoebel effect is finite, they simply multiply the current by the quantity $S_c=\ell_s/(\ell_s+a)$, which goes to zero if $\ell_s=0$ (no Schwoebel effect) and it is $S_c=1$ for an infinite Schwoebel effect.

If expression (3.2) were the only contribution to the current, a smooth surface should be unstable with respect to height fluctuations of any wavelength. This prediction may be tested by simulations on a sample of small size λ with periodic boundary conditions. These simulations, reported in Secs. V and VIII [respectively, in the cases of deterministic (DN) and random nucleation (RN)], show that the surface remains smooth if λ is not too large. Consequently, the flat surface is stable with respect to height fluctuations of short wavelength and (3.2) must be corrected. As recalled in Sec. I, the usual correction[3,8,15,19] is an additional, linear term which should be of third order for symmetry reasons. The physical meaning of this term will be discussed in the next section. The resulting equation reads

$$j=\frac{F\ell_s\ell_c m}{2(1+|m|\ell_s)(1+|m|\ell_c)}+K\frac{\partial^2 m}{\partial x^2}. \tag{3.3}$$

This expression will be seen to be satisfactory for *weak slopes*. The linearized form of (3.3), valid for small values of m, is

$$j=\frac{F}{2}\ell_s\ell_c m+K\frac{\partial^2 m}{\partial x^2}. \tag{3.4}$$

Inserting this equation into (1.1), for each Fourier component $[z(x,t)=z_q(t)\exp(iqx)]$, one finds

$$\frac{\partial z_q}{\partial t}=a\left(\frac{F\ell_s\ell_c}{2}q^2-Kq^4\right)z_q. \tag{3.5}$$

The expression in brackets is negative for $q>q^*=\sqrt{F\ell_s\ell_c/2K}$, so that a flat surface is stable with respect to height fluctuations of wavelength smaller than

$$\lambda_c^{\inf}=\frac{2\pi}{q^*}=2\pi\sqrt{\frac{2K}{F\ell_s\ell_c}}. \tag{3.6}$$

The instability appears after a time of order

$$t^*\approx\frac{1}{aF\ell_s\ell_c(q^*)^2}\approx\frac{K}{a(F\ell_s\ell_c)^2} \tag{3.7}$$

so that

$$\lambda_c^{\inf}\approx\sqrt{aFt^*\ell_s\ell_c}. \tag{3.8}$$

This formula has already been obtained by Krug.[27]

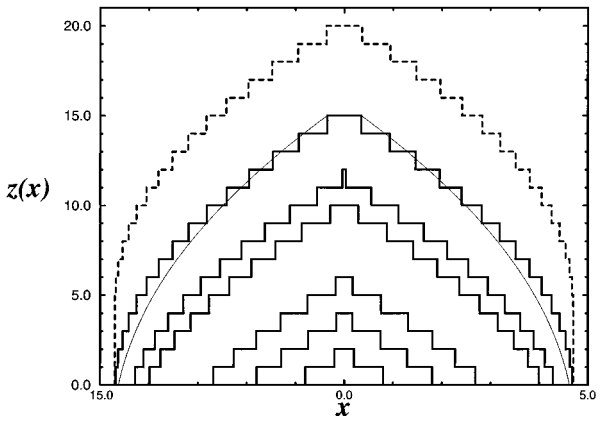

FIG. 2. Stationary configurations (thick lines) for different wavelengths ($\lambda/\ell_c=2,4,6,8,8.6,9.397$) and unstable configuration (dashed line) for $\lambda/\ell_c=9.4$. The thin line represents the analytical profile (6.12). Deterministic nucleation, $\ell_s/\ell_c=0.015$.

IV. MEANING AND VALUE OF THE STABILIZING FORCE *K*

The linear term in (3.3) is generally supposed to represent the thermal smoothing arising from exchange of atoms between terraces. However, we claim (in contrast with Ref. 12) that it can also represent the effect of stochastic formation of new terraces, at least at short times. At longer times, when the surface profile has acquired a patterned structure, the linear term fails to account for the fact that new terraces do not nucleate uniformly, but preferably near maxima.

Neglecting thermal smoothing, K can be estimated in the limit of the vanishing Schwoebel effect. Then (2.12) holds, and since $[K]=\text{length}^3/\text{time}$, comparison with (1.1) yields

$$K\approx F\ell_c^4. \tag{4.1}$$

Insertion into (3.6) yields

$$\lambda_c^{\inf}\approx\ell_c\sqrt{\frac{\ell_c}{\ell_s}}. \tag{4.2}$$

These results rely on Eq. (3.3), in which the linear term is purely phenomenological. It is therefore of interest to test (3.3). This test can be done on samples of small size λ, but slightly larger than $\lambda_c^{\inf}$. The simulations reported in the next sections and in Appendix A 1 and A 2 show that such samples evolve toward a stationary shape (Figs. 2 and 6). Is such a stable stationary shape predicted by (3.3) as well? This is a crucial test of (3.3).

For a slightly different current [the first term of (3.3) being replaced by (1.4)], Hunt *et al.*[19] have shown that stationary mounds are obtained for all $\lambda>\lambda_c^*=2\pi\ell_d$ [see Eq. (1.4) for the meaning of ℓ_d]. Their calculation has been extended to (3.3) in Appendix B and an analogous result is found. Anyway, the actual form of the mounds—as obtained from our simulations—is rather different from the analytical shape predicted by (3.3).

V. STATIONARY PROFILES: NUMERICAL SOLUTION OF THE DETERMINISTIC ZENO MODEL

We have solved the ''Zeno'' equations (2.5)–(2.9) for an initial state in which all terraces have the same width $\ell(0)<\ell_c$. In this section, new terraces will be assumed to be nucleated at the center of an old one, when its width becomes equal to ℓ_c. This *deterministic* nucleation scheme has the advantage to give fully reproducible results, independent of any fluctuation. The computer is used as a tool to solve difficult equations, not to make simulations. The results will turn out to be partly applicable to the case of random nucleation. Details are given in Appendix A 1. The main results are as follows (see Fig. 2).

(i) For periods λ smaller than a certain length $\lambda_c^{\sup}$ and larger than $\lambda_c^{\inf}=\ell_c$, the profile—if averaged on a time much larger than $1/aF$—evolves toward a well-defined, nontrivial shape. This shape is therefore a stable fixed point of the evolution equations, and the height of the profile increases with λ.

(ii) The minima of the stationary structures are angular points.

(iii) Far from a minimum, all stationary profiles may be approximated by a ''universal'' curve which is independent of λ, but does depend on ℓ_c and ℓ_s.

(iv) If $\lambda>\lambda_c^{\sup}$ the height difference δz between minima and maxima becomes always deeper, at increasing time.

(v) The transition from regime (i) to regime (iv) is discontinuous, i.e., δz jumps abruptly from a finite value to infinity for $\lambda=\lambda_c^{\sup}$.

Of course, statement (iii) makes sense only if

$$\lambda \gg \ell_c \tag{5.1}$$

and this equation can only be satisfied if

$$\ell_c \gg \ell_s . \tag{5.2}$$

As will be seen, some of these results can be obtained analytically in the continuum approximation, and the ''universal'' shape can be found.

VI. STATIONARY PROFILES: CONTINUUM APPROXIMATION

The calculation will be made for negative values of the profile slope $m=\partial z/\partial x$ (see Fig. 1). The condition $|m|\ell_c>1$ will be assumed. Let v_n be the velocity of the nth step and ℓ_n the width of the terrace, between x_{n-1} and x_n. Defining

$$\delta x_n(t,1/aF)=x_n(t+1/aF)-x_n(t)=\int_t^{t+1/aF} dt' v_n(t') \tag{6.1}$$

the stationarity condition for vicinal terraces, ignoring possible nucleation of new terraces, writes

$$\delta x_n(t,1/aF)=\ell_{n+1}(t). \tag{6.2}$$

Substituting $v_n(t)$ by its expression (2.5), (6.1) reads

$$\delta x_n(t,1/aF)=\int_t^{t+1/aF} dt'\{f[\ell_n(t')]+g[\ell_{n+1}(t')]\}. \tag{6.3}$$

We make the approximation

$$\ell_n(t')\simeq \frac{\ell_n(t)+\ell_n(t+1/aF)}{2}\simeq \frac{\ell_n(t)+\ell_{n+1}(t)}{2}. \tag{6.4}$$

Integration yields

$$\delta x_n(t,1/aF)=\frac{1}{aF}\left\{ f\left(\frac{\ell_n+\ell_{n+1}}{2}\right)+g\left(\frac{\ell_{n+1}+\ell_{n+2}}{2}\right)\right\}. \tag{6.5}$$

If all the terraces have the same length ℓ, the above equations are fulfilled for every value of ℓ. In general, let us define $\ell'=(\ell_n+\ell_{n+1})/2$ and $\ell''=(\ell_{n+1}+\ell_{n+2})/2$; by using formulas (2.6) and (2.7) for f and g, the above equation reads

$$\delta x_n(t,1/aF)=\frac{\ell'+\ell''}{2}+\frac{\ell_s^2(\ell''-\ell')}{2(\ell_s+\ell')(\ell_s+\ell'')} \tag{6.6}$$

or

$$\delta x_n(t,1/aF)-\ell_{n+1}=\frac{1}{2}\left[\ell'+\ell''-2\ell_{n+1}+\frac{\ell_s^2(\ell''-\ell')}{(\ell_s+\ell')(\ell_s+\ell'')}\right]. \tag{6.7}$$

Replacing $(\ell''-\ell')$ and $(\ell''+\ell'-2\ell_{n+1})$ by their Taylor expansion, one obtains for negative values of the local slope $m(x)\equiv 1/\ell(x)$

$$\delta x_n(t,1/aF)-\ell_{n+1}=-\frac{1}{m}\frac{\partial}{\partial x}\left[-\frac{\ell_s}{2(1+\ell_s m)}+\frac{1}{4m^3}\frac{\partial m}{\partial x}\right]. \tag{6.8}$$

This quantity is the shift δx of the profile in the x direction during the time $1/(aF)$. In the continuum approximation it may be written as

$$\delta x=\frac{1}{aF}\frac{\partial x}{\partial t}=\frac{1}{aFm}\frac{\partial z}{\partial t}=-\frac{1}{mF}\frac{\partial j}{\partial x}. \tag{6.9}$$

The current density is therefore equal to

$$j=\frac{F\ell_s}{2(1+\ell_s|m|)}\frac{m}{|m|}+\frac{F}{4m^3}\frac{\partial m}{\partial x}\equiv j_s+j_c, \tag{6.10}$$

where the factor $m/|m|$ has been introduced in order to take both possibilities $m<0$ and $m>0$ into account.

The first term reproduces expression (3.2) in the limit $|m|\ell_c\gg 1$ [see also Eq. (3.1)] and corresponds to the Schwoebel current j_s. It is destabilizing. The second contribution (j_c)—which breaks the up-down symmetry—derives from a curvature in the surface profile and in the regions of negative curvature ($\partial_x m<0$), j_c and the slope m have opposite signs, so that j_c is stabilizing.

It is rather remarkable that j_c does not depend on ℓ_s. Its origin may be understood by considering the evolution of the

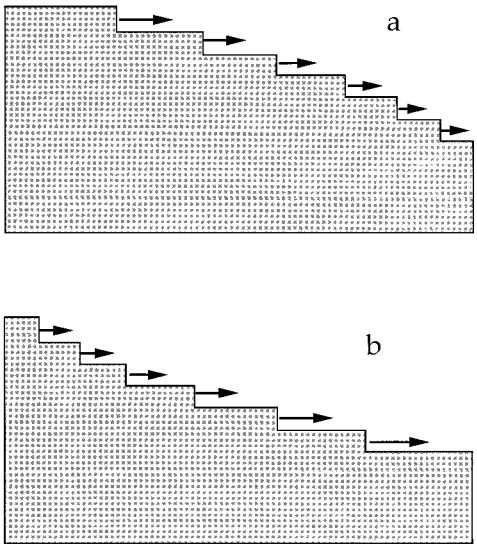

FIG. 3. Small pieces of a vicinal surface. The arrows indicate the velocity of each step. The slope m is negative in both cases, but the curvature $\partial_x m$ is negative in (a) and positive in (b).

two profiles of Fig. 3, in absence of the Schwoebel effect. In the case (a) $m<0$ and $\partial_x m<0$, while in (b) $m<0$ and $\partial_x m>0$. If $\ell_s=0$, the velocity of each step is proportional to the sum of the lengths of the upper and lower terrace. So, in (a) larger terraces become smaller while in (b) their size increases. Briefly, j_c explains why a growing vicinal surface is not stationary if neighboring terraces have different sizes ($\partial_x m\neq 0$).

Coming back to the case of negative slopes, the stationarity condition $j=0$ writes

$$-\frac{F\ell_s}{2(1+\ell_s|m|)}+\frac{F}{4}\frac{1}{m^3}\frac{\partial m}{\partial x}=0, \tag{6.11}$$

which can be easily integrated. Assuming that the curve has the initial slope $m(0)=-m_0$, we obtain

$$z(x)=z(0)+\frac{1}{4}\ln[y(1+2\ell_s m_0)]+\frac{1}{2\ell_s m_0}[\sqrt{m_0^2\ell_s^2+y^2}-(1+\ell_s m_0)]-\frac{1}{2}\ln\left\{\frac{\sqrt{m_0^2\ell_s^2+y}+m_0\ell_s}{\sqrt{m_0^2\ell_s^2+y}-m_0\ell_s}\right\} \tag{6.12}$$

with $x>0$ and

$$y=1+2\ell_s m_0-4\ell_s m_0^2 x. \tag{6.13}$$

The other half of the curve ($x<0$) is easily obtained by symmetry. A remarkable property of the curve (6.12) is to be limited by two vertical asymptotes; because of this, a maximal value for the wavelength of a stationary configuration will be seen to exist. This finding contrasts with the analogous curve deduced from (3.3)—and derived in Appendix B—or with the results of Hunt *et al.*[19]

In the above calculation, maxima and minima have been disregarded. In this section, as in the preceding one, new terraces will be assumed to be nucleated at the center of the top terrace when its width becomes equal to ℓ_c. In this deterministic model, what happens at a maximum? The width of the top terrace fluctuates between 0 and ℓ_c and its average length should be close to $\ell_c/2$. The width of the terraces just below is exactly $\ell_c/2$ just after the latest nucleation, and should not change much if (5.2) is satisfied. More generally, the highest terraces have a width close to $\ell_c/2$. Therefore the slope at the top of the profile is close to $2/\ell_c$. This means that in (6.12) one has $m_0=2/\ell_c$. The top of the profile is seen to be an angular point, however with an angle close to π [see Fig. 2(a)]. This will be shown to be an artefact of the deterministic nucleation model.

What occurs now at minima? Numerical treatment suggests that the steady profiles are well approximated by arcs of a universal curve, which is obviously given by (6.12), connected by angular points. In fact, if we impose the stationary condition to the case of a bottom terrace and the approximation (6.4) is made, we find that a stationary profile corresponds exactly to the vanishing of the current (6.10). Strictly speaking, Eq. (6.2) would imply $j=$const, but the constant is not zero only on a vicinal surface: if the average slope of the substrate is zero, it *must* be zero.

Anyway, approximation (6.4) is not satisfactory for a bottom terrace, whose size changes a lot during the filling time of a layer. It is just for this reason that our analytical treatment fails in the explanation of property (v) of Sec. V, according to which, for a given value of ℓ_s/ℓ_c, the height δz of a stationary profile has a finite upper limit. This may be understood as a result of the Zeno paradoxon in its Elkinani-Villain version:[18] if very low values of the terrace width $\ell\ll\ell_s$ were allowed at the bottom of the profile, the Schwoebel effect could be considered infinite and the depth would increase to infinity (or, in practice, up to a value of order λ/a).

Equation (6.13) for y makes sense only if x is smaller than a critical value $x_{\max}$, where y vanishes. More precisely, $z(x)$ has two vertical asymptotes for $x=\pm x_{\max}$. This upper bound yields an evaluation of $\lambda_c^{\sup}=2x_{\max}$, namely

$$\lambda_c^{\sup}=\frac{\ell_c^2}{8\ell_s}+\frac{\ell_c}{2}. \tag{6.14}$$

The validity of our expression (6.10) for the current can be tested by comparing the analytical expressions for the profile $z(x)$ [Eq. (6.12)] and for the upper critical wavelength $\lambda_c^{\sup}$ [Eq. (6.14)], with the numerical results. In Fig. 2(a) stationary profiles are seen not to depend very much on the wavelength and they are also well fitted by the ''universal curve'' $z(x)$. This is a good surprise, because the current (6.10) is an arbitrary cut at the term in $\partial_x m$.

In Fig. 4 we report the numerical and analytical values for $\lambda_c^{\sup}(\ell_s)$. Again, the good agreement proves that a continuum approach is essentially correct.

VII. GENERAL PROPERTIES OF STATIONARY STRUCTURES

The two preceding sections suggest that the steady solutions of the deterministic Zeno equations which are periodic with one maximum per period, have with a good approximation the following two properties (Fig. 2 and Fig. 5).

(i) Between two minima, they have a universal shape

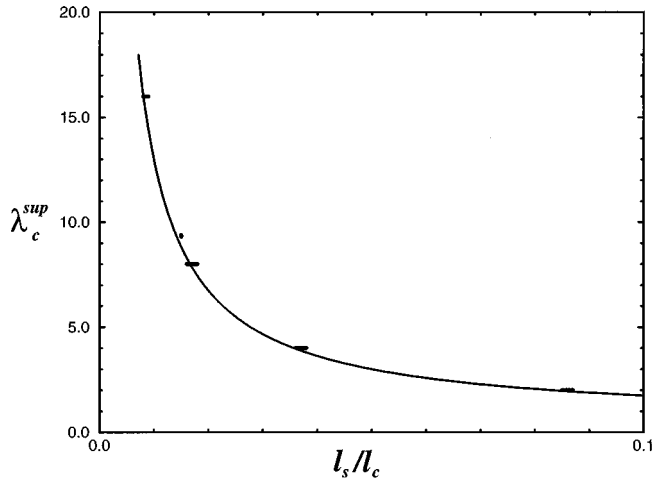

FIG. 4. Numerical (bars) and analytical (curve) values of $\lambda_c^{\sup}(l_s/l_c)$.

$$z(x)=z_n+\varphi_0(x-x_n), \tag{7.1}$$

where $\varphi_0(x)$ is a universal function and the constant x_n changes at each minimum. The constant z_n is the same everywhere, but the index n has been introduced for future use. This property will be called *rule of universal shape* in the following.

(ii) Each minimum is an angular point where the slope has the same absolute value on both sides. This property will be called *rule of equal slopes* in the following, and it is a trivial consequence of periodicity, symmetry, and the rule of universal shape.

Since all minima ignore one another, any structure which satisfies rules (i) and (ii) is stationary [Fig. 5(b)]. These structures have the remarkable property that all maxima have equal heights. They will probably not be obtained in the evolution of an initially planar surface, and therefore they have no particular interest. What is interesting is that, as argued below, there is *no* other nontrivial stationary structure.

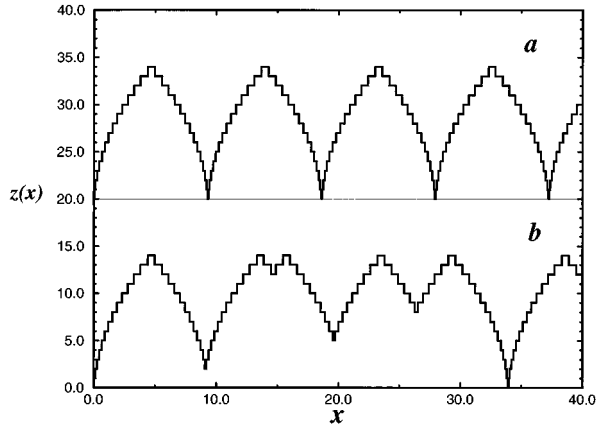

FIG. 5. Stationary solutions of the Zeno equations. (a) A periodic solution. (b) A nonperiodic solution, made of pieces of the universal curve.

VIII. PERIODIC, STATIONARY PROFILES WITH RANDOM NUCLEATION

In Sec. V deterministic rules have been assumed for the nucleation of new terraces. This is not realistic, but should provide a good description of the minima because nucleation is not expected to be frequent there.

We have also done simulations using the RN scheme, on samples of small size λ, which can be regarded as a period since periodic boundary conditions are imposed. In contrast with the case of deterministic nucleation, the results do not depend on the initial state, so that it is not essential to take a single maximum per period at the beginning of the simulation; even, we can take a flat configuration at $t=0$. The following study should also allow, by comparing the results with formula (3.6), to determine the parameter K, which enters in the current (3.3).

The simulations are described in detail in Appendix A 2 and show the following properties. (i) For periods λ smaller than a certain length $\lambda_c^{\sup}$, *but larger* than another length $\lambda_c^{\inf}$, the profile evolves toward a well-defined, nontrivial shape (Fig. 6). (ii) The minima of the stationary structures are angular points. (iii) Far from a minimum, all stationary profiles may be approximated by a λ-independent, ''univer-

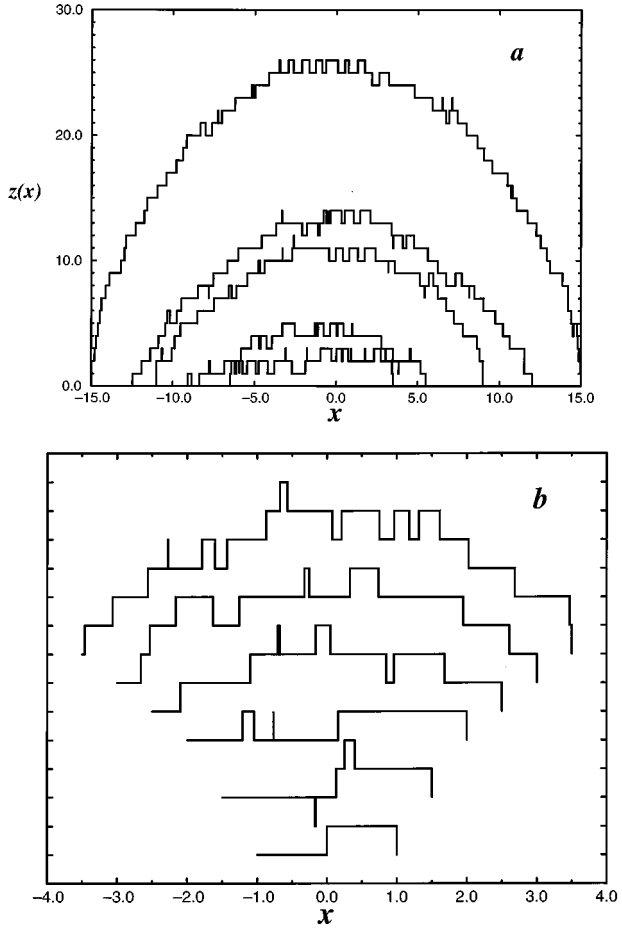

FIG. 6. (a) Stationary configurations for different wavelengths ($\lambda/l_c=10,15,20,25,30$). Random nucleation, $l_s/l_c=0.015$. (b) Asymptotic configurations at different wavelengths ($\lambda/l_c=2,3,4,5,6,7$). Random nucleation, $l_s/l_c=0.06$. The lower critical wavelength can be located in between $4l_c$ and $5l_c$.

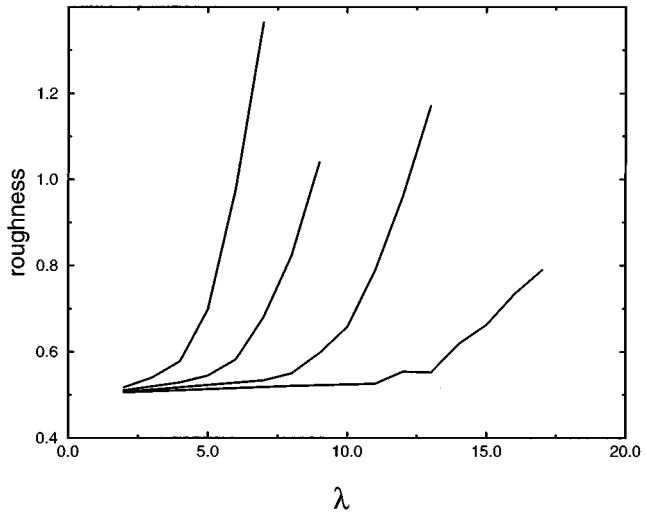

FIG. 7. Average roughness of the asymptotic configurations of small samples, as a function of the wavelength, for different values of the Schwoebel length: from the left to the right, $\ell_s/\ell_c = 0.06, 0.03, 0.015, 0.0075$. Random nucleation.

sal'' curve, however rather different from the universal curve of the deterministic case. (iv) If λ is larger than $\lambda_c^{\rm sup}$, but not too much larger (let us say, smaller than $2\lambda_c^{\rm sup}$), the height difference δz between minima and maxima becomes always deeper. (v) The transition from regime (i) to regime (iv) is discontinuous. (vi) If λ is much larger than $\lambda_c^{\rm sup}$, additional minima appear. (vii) The top of the profile is fairly flat, and $\lambda_c^{\rm sup}$ is much larger than the corresponding value, obtained with deterministic nucleation.

In both deterministic and random models, we have defined a lower ($\lambda_c^{\rm inf}$) and an upper ($\lambda_c^{\rm sup}$) critical wavelength. A nontrivial steady configuration is found only for $\lambda_c^{\rm inf} < \lambda < \lambda_c^{\rm sup}$ For smaller values we have a flat surface and for larger ones, an instability takes place with the formation of deep crevaces. The numerical values of $\lambda_c^{\rm sup}$ are different in the two models, but randomness probably does not introduce new phenomena: a deterministic model is sufficient to understand the origin of the ''upper'' instability. At variance, $\lambda_c^{\rm inf}$ has some sense only in the random model, since in the deterministic one $\lambda_c^{\rm inf} = \ell_c$ and its introduction is not meaningful.

The dependence $\lambda_c^{\rm inf} \sim \ell_s^{-1/2}$ expected from (4.2) can be tested numerically. In Fig. 7 we report, for different values of the Schwoebel length, the average roughness of the ''stationary'' configurations, obtained for samples of different wavelength. We see that for small L, roughness is constant and does not depend on ℓ_s, while for larger values of L (depending on ℓ_s) it increases rather rapidly. The transition between the two regimes defines the lower critical wavelength. Even though its location is somewhat ambiguous, the expected dependence (4.2) seems to agree with our numerical results, with a numerical prefactor of order 1. The reason of the difficulty in defining $\lambda_c^{\rm inf}$ is presumably that there is a smooth crossover, rather than a sharp transition between the two regimes.

The growing surfaces which are obtained from simulations on large samples are not stationary, but their evolution

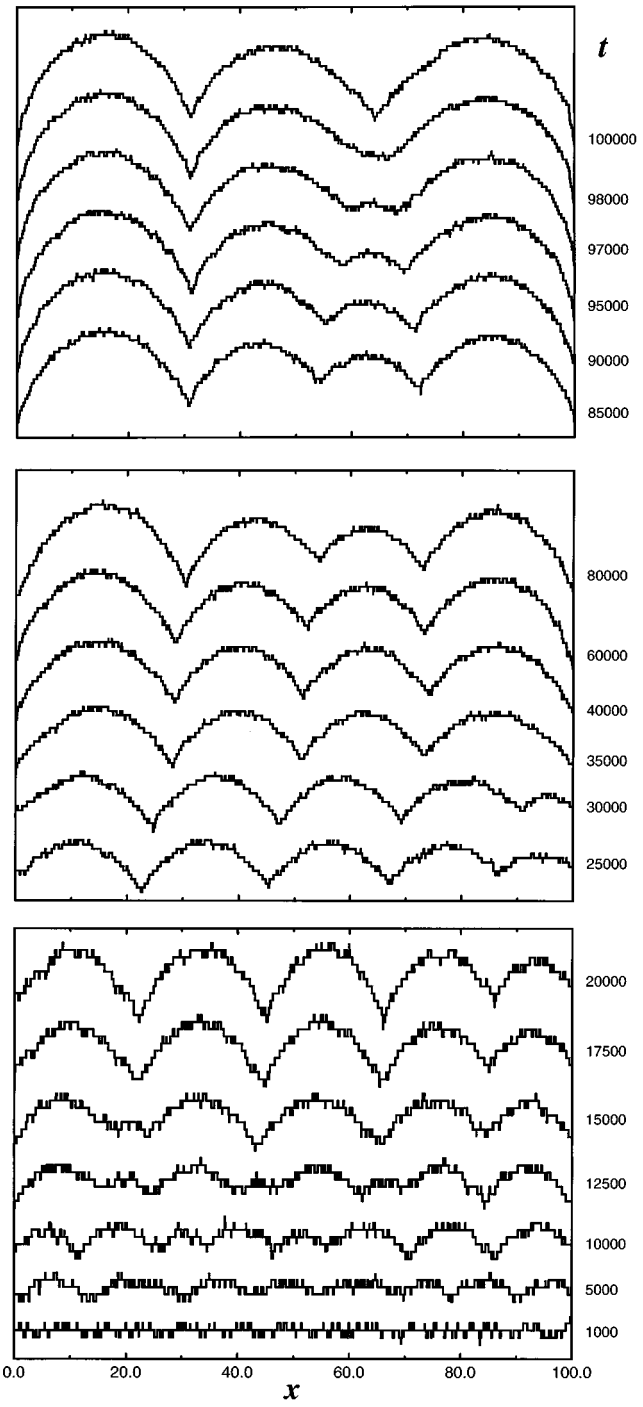

FIG. 8. Configurations at increasing times, of a large sample ($\lambda/\ell_c = 100$). Random nucleation, $\ell_s/\ell_c = 0.015$. The number of deposited layers is indicated on the right.

is slow and they can be called ''quasistationary'' (Fig. 8). In addition, they are made of mounds of similar size, and in this sense they are not far from being periodic. The stationary, periodic structures which emerge from the numerical treatment may be roughly described by the same two properties, enounced at the beginning of Sec. VII.

Since no analytical expression is available for $\lambda_c^{\rm sup}$, we have not drawn the analogous of Fig. 4 for random nucleation. For some specific values of ℓ_s, we find that (ℓ_c is the unit length): $\lambda_c^{\rm sup}(\ell_s = 0.06) = 8/8.5$, $\lambda_c^{\rm sup}(\ell_s = 0.03) = 15/16$

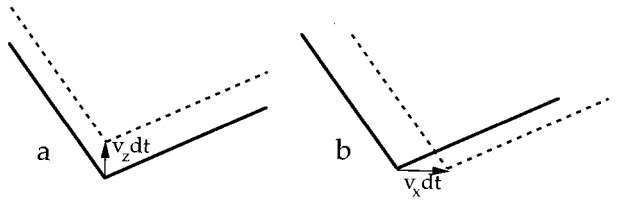

FIG. 9. Evolution of the profile near an angular point (a) if $v_x=0$ and (b) if $v_z=0$.

and $\lambda_c^{\rm sup}(\ell_s=0.015)=30/32$. These results are in agreement with a dependence of the form $\lambda_c^{\rm sup}\sim 1/\ell_s$.

IX. ANGULAR POINTS IN THE (1+1)-DIMENSIONAL PROBLEM

Simulations suggest that the minima of the profile are angular points. These angular points move. Let $\vec{v}$ be the velocity of an angular point. If $v_x=0$ [Fig. 9(a)], we obviously have $\partial z/\partial t=v_z$; if $v_z=0$ [Fig. 9(b)], we have $|\partial z/\partial t|=|mv_x|$, where $m=\partial z/\partial x$. To clarify the sign one can see that, if $v_x>0$ (<0), then $\partial z/\partial t$ is positive (negative) and m negative on the left of the minimum, while $\partial z/\partial t$ is negative (positive) and m positive on the right. Thus, in both cases $\partial z/\partial t=-mv_x$. Adding the contributions proportional to v_x and v_z, one obtains near a minimum

$$\frac{\partial z}{\partial t}=v_z-mv_x \tag{9.1}$$

and therefore

$$a\frac{\partial j}{\partial x}=mv_x-v_z. \tag{9.2}$$

The same result can be obtained by writing

$$z(x)=z(x_a)+\int_{x_a(t)}^{x}dx'\,\frac{\partial z}{\partial x'}, \tag{9.3}$$

where $x_a(t)$ means the angular point. The time derivative gives

$$\frac{\partial z(x,t)}{\partial t}=v_z-v_x m(x_a,t)+\int_{x_a(t)}^{x}dx'\,\frac{\partial}{\partial t}\,\frac{\partial z(x',t)}{\partial x'} \tag{9.4}$$

and by writing $\partial_t z=-a\partial_x j$ on both sides, Eq. (9.2) is recovered.

X. NATURE AND WEAKNESS OF A LOCAL PHENOMENOLOGICAL EQUATION OF MOTION

The Zeno equations (2.5)–(2.9), which define the deterministic motion of steps are too complicated to provide insight into the evolution mechanism. We now look for a phenomenological differential equation in the continuum approximation. A local form, natural generalization of (1.2), might be

$$j(x,t)=\varphi[m(x,t),m'(x,t),m''(x,t)], \tag{10.1}$$

where $m=\partial z/\partial x$, $m'=\partial^2 z/\partial x^2$ and $m''=\partial^3 z/\partial x^3$.

The local current φ should contain the following.

(i) An m-dependent term, representing the nonequilibrium current, mainly due to the Schwoebel effect. Its expression is given in Eq. (3.2) and it is derived in Appendix B. In the absence of nonthermal healing mechanisms[16,17] and if the crystal structure is not taken into account,[15] it is always positive and only vanishes for $m=0$ or $m=\infty$.

(ii) A current which breaks the up-down symmetry $[z(x)\to -z(x)]$. Such a term has been introduced phenomenologically by several authors[28–30,12] who assumed that, for weak slopes, it has the form const$\times\partial_x(m^2)$. On the other hand, for $|m|\ell_c\gg 1$, Eq. (6.10) shows that the current contains a contribution of order $[F(\partial_x m)/m^3]$. It is plausible to assume that both forms match for $|m|\ell_c\approx 1$, so that the contribution of interest to the current is[31]

$$\frac{Fc_1\ell_c^4}{(c_2+m^2\ell_c^2)^2}\,\frac{\partial(m^2)}{\partial x}=-\frac{\partial}{\partial_x}\left[\frac{Fc_1\ell_c^2}{c_2+m^2\ell_c^2}\right]\equiv-\frac{\partial A(m^2)}{\partial x}, \tag{10.2}$$

where the positive constants c_1 and c_2 are of order unity. In the deterministic model where (6.10) applies, $c_1=1/8$.

(iii) A term containing $m''=\partial^2 m/\partial x^2$. As discussed in Sec. III, it can result both from exchange of atoms between steps and from terrace nucleation. In our model, the first contribution is ignored. On the other hand, terrace nucleation becomes negligible when the terrace size is much smaller than ℓ_c. This property can be accounted for if the term Km'' of formula (3.3) is multiplied by a function $\theta(m,m')$ which vanishes when nucleation is not expected, i.e., for $|m|\ell_c\gg 1$, or should vanish for too large, *positive* values of m', namely $m'\ell_c^2\gg 1$. For $m'<0$ and $|m|\ell_c\ll 1$, the function $\theta(m,m')$ is equal to 1.

In conclusion, the most general local form of the current is

$$\varphi(m,m',m'')=\frac{F\ell_c\ell_s m}{2(1+\ell_s|m|)(1+\ell_c|m|)}-\frac{\partial A(m^2)}{\partial x}+Km''\theta(m,m'). \tag{10.3}$$

The numerical work reported in Sec. VIII suggests that, after some time, the minima of the profile are angular points. This is in agreement with the analytic study of Sec. VI, where the first two terms of (10.3) are shown to produce a current which carries matter away from a minimum $(m=0,m'>0)$.

Now, if there is an angular point, the current density $j(x,t)$ cannot be given by Eq. (10.3) in its neighborhood, since this current would be discontinuous and a δ-function singularity would arise in the profile.

The best *way* to reconcile our dream of a continuous equation with the reality of angular points is a nonlocal form.

XI. NONLOCAL EQUATION OF MOTION

There is no reason to expect a continuous, local equation of motion to describe the model. Indeed a continuum model can only be valid for an averaged surface, since the real surface has steps and is therefore not continuous. The surface has to be averaged on a length of order ℓ (the distance between steps) and on a time of order $1/(Fa)$. The resulting

equation of motion has to take into account what happens during this time in a range of order ℓ around each point. Therefore, the effective equation of motion, resulting from the integration of the microscopic equations (2.5)–(2.10) on a time of order $1/(Fa)$, has no reason to be local. Away from a minimum, the approximation (6.4) transformed the problem into a local one. However, as already pointed out, this approximation is too rough for a bottom terrace, whose size changes a lot in time. For this reason, a local approximation may fail near a minimum, and it does fail in our model.

We do not claim that any local, continuous growth equation is incompatible with angular points. For instance, the deterministic Kardar, Parisi, Zhang equation:[32]

$$\frac{\partial z}{\partial t}=\nu m'+\frac{\lambda}{2}m^2 \tag{11.1}$$

is known to give rise to angular points,[32] at least if $\nu=0$. However, if the expression of $\partial z/\partial t$ contains $\partial^2 z/\partial x^2=m'$ or higher derivatives, this expression becomes infinite at an angular point, and angular points can become impossible. In the problem of interest in the present paper, $\partial z/\partial t$ involves only terms containing m' or higher derivatives and a nonlocal form is unavoidable as argued above—at least if θ vanishes in the last term of (10.3).

We will assume that the current satisfies a nonlocal, phenomenological equation of the form

$$j(x,t)=\int_{-\infty}^{+\infty}\Gamma(x-u)\varphi(m(u,t),m'(u,t)m''(u,t))du. \tag{11.2}$$

The function $\Gamma(u)$ is different from 0 in a small interval ε^{-1} around $u=0$, and its integral is equal to 1. Moreover, symmetry implies that $\Gamma(u)$ is even. A natural guess is

$$\Gamma(u)=\frac{\varepsilon}{2}\exp(-\varepsilon|u|), \tag{11.3}$$

where ε^{-1} will be seen to be of order ℓ_c.

Far from an angular point, the function $\varphi(x)$ can be assumed constant on the domain where $\Gamma(u-x)$ is different from 0, so that $\varphi(m,m',m'')$ can be identified with (10.3). It can also be seen that $\Gamma(u)$ should be even, otherwise the local approximation of (11.2) would contain the product of m' by an even function of m, which is forbidden by symmetry.

In order to check that (11.3) is an appropriate guess, we now consider the vicinity of angular points. Neglecting K in (10.3), one obtains

$$\varphi(m,m',m'')=\frac{F\ell_c\ell_s m}{2(1+\ell_s|m|)(1+\ell_c|m|)}-\frac{\partial A(m^2)}{\partial x}, \tag{11.4}$$

where the function $A(m^2)$ has been defined in (10.2) and whose deterministic limit is $F/(8m^2)$.

As seen from (9.2), $\partial j(x,t)/\partial x$ is generally a discontinuous function of x at a minimum, but $j(x,t)$ must be continuous. Now, the leading singularity of the current (11.2) results from the leading singularity of (11.4), which is due to its second term and it is a δ type singularity. The most singular term of (11.4) near an angular point at $x=\xi$ is indeed

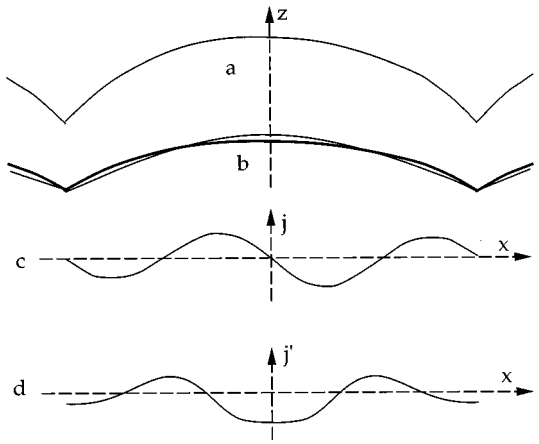

FIG. 10. Evolution of a periodic profile according to (11.2). (a) Stationary profile. (b) Initial profile smoother than the stationary one, and affine to it (thick line). (c) Resulting current of atoms. (d) Resulting current gradient $j'=\partial j/\partial x$. As a consequence of the equation $\partial z/\partial t=-j'$, the profile takes the form shown by the thin line in (b), for which the current is now uniformly destabilizing.

$$\varphi_{\text{sing}}(m(u,t),m'(u,t))=-\Delta(A(m^2))\delta(u-\xi(t)), \tag{11.5}$$

where $\Delta(A)\equiv A_r-A_l$ means the discontinuity of A, across the angular point (r and l stand, respectively, for *right* and *left*). For the deterministic model, $\Delta(A(m^2))=(F/8)\Delta(1/m^2)$.

Insertion of (11.5) into (11.2) yields the most singular part of the current density:

$$j_{\text{sing}}(x,t)=-\Delta(A(m^2))\int_{-\infty}^{+\infty}\Gamma(x-u)\,\delta(u-\xi(t))du \tag{11.6}$$

or

$$j_{\text{sing}}(x,t)=-\Delta(A(m^2))\Gamma(x-\xi(t)). \tag{11.7}$$

According to (9.2), this current should be continuous and have a discontinuous derivative at $x=\xi$. It follows from (11.7) that $\Gamma(u)$ must have the same properties. The form (11.3) has indeed these properties.

We can now ask how the previous description is modified if the relaxation term (Km'') is added to the local current (11.4). In this case the strongest singularity in $\varphi(m,m',m'')$ is not eliminated by the spatial integration (11.2) and even the nonlocal current j would be discontinuous. This means that if the term (Km'') is present, there are no angular points. However, our simulations do show angular points, so that such a term must be negligible close to them.

As a first test of Eq. (11.2), let us consider the evolution of a periodic profile which is initially smoother than the stationary shape $z_0(x)$. Let us assume, for instance, $z(x,t=0)=\lambda z_0(x)$, with $\lambda<1$ [Fig. 10(b)]. Near a maximum, Eq. (3.3) holds and the stabilizing second term is more reduced than the destabilizing first term, so that the current of atoms is directed toward the top. Near a minimum, but not too close, Eq. (6.10) holds and the stabilizing second term is increased, so that the current of atoms is directed toward the bottom. Very close to a minimum, the integral equation

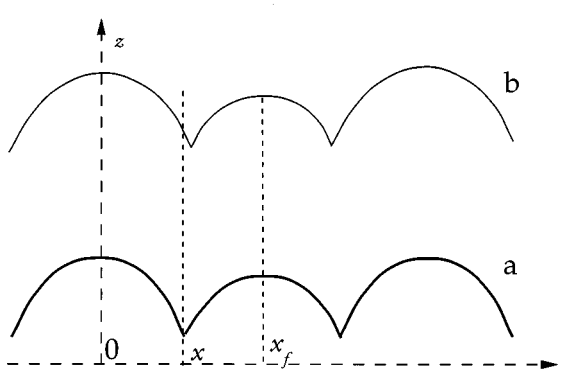

FIG. 11. The larger mounds eat the smaller one, in the center. Points $x=0$ and $x=x_f$ do not move, because of the symmetry. (a) $t=0$; (b) $t>0$.

(11.2) has to be used, so that the current is continuous at the minimum. Symmetry implies that it vanishes. It results that the current has the shape shown in Fig. 10(c).

The modification $\partial z/\partial t=-\partial j/\partial x$ [Fig. 10(d)] of the profile follows: initially, both maxima and minima go up. However, the slope near the minima becomes flatter as seen from Fig. 10(b), in other words m' becomes weaker, so that the current, as given by (11.2) very close to a minimum, or by (6.10) a little farther, changes sign, as well as j'. To summarize, the velocity of the minima is positive in the transient, initial state, but then become negative, so that the profile shape tends to the ''universal'' shape $\varphi=0$ in agreement with simulations.

XII. VELOCITY OF ANGULAR POINTS

In this section, the velocity of angular points will be related to the discontinuity of the slope and of the curvature, using Eq. (11.2). From (11.7) one deduces the discontinuity of the current density gradient

$$\Delta\left(\frac{\partial j(x,t)}{\partial x}\right)=-\Delta\left(\left.\frac{\partial\Gamma}{\partial x}\right|_{\xi}\right)\Delta(A(m^2)). \tag{12.1}$$

According to (9.2), this should be equal to $\Delta(m)(v_x/a)$. Therefore

$$v_x=-a\Delta\left(\left.\frac{\partial\Gamma}{\partial x}\right|_{\xi}\right)\frac{\Delta(A(m^2))}{\Delta(m)}. \tag{12.2}$$

If Eq. (11.3) is assumed, we obtain

$$v_x=a\varepsilon^2\frac{\Delta(A(m^2))}{\Delta(m)}. \tag{12.3}$$

The comparison of this formula with numerical results tells that $\varepsilon^{-1}\sim l_c$.

The main consequence of (12.2) [or (12.3)] is that a minimum moves in the direction where the absolute value of the slope is weaker. In particular, if—as in Sec. IX—one considers a profile which initially satisfies the condition $j=0$ everywhere between angular points (Fig. 11), one finds that the smaller arcs of the universal curve shrink (as long as they do not exceed the critical value $\lambda_c^{\sup}$). If $m_r=-m_l$, (12.2) predicts that $v_x=0$ in agreement with the rule of equal slopes.

An interesting case is that of an angular point where the slopes have the same sign on both sides. According to (12.2), such an angular point has a positive horizontal velocity, if both the slopes are negative. This is in agreement with the numerical results of Ref. 18, according to which such a step bunch moves downward. Anyway, a step bunch should be represented by a discontinuity in the surface profile $z(x)$, so that the current itself $j(x)$ should be discontinuous across it.

Now we want to calculate the vertical component of the velocity of the angular point, v_z. By evaluating (9.2) on both sides of the angular point, we can write

$$v_z=-\frac{\Delta\left(\frac{a}{m}\frac{\partial j}{\partial x}\right)}{\Delta\left(\frac{1}{m}\right)}. \tag{12.4}$$

The singular part of the current is such that its spatial derivative changes sign across $x=\xi$; on the contrary, the nonsingular part ($j_{\rm ns}$) of the current gives a continuous contribution to $\partial_x j$. So, we can write

$$\left.\frac{\partial j}{\partial x}\right|_{\xi^{\pm}}=\frac{\partial j_{\rm ns}}{\partial x}-\left.\frac{\partial\Gamma}{\partial x}\right|_{\xi^{\pm}}\Delta(A(m^2)). \tag{12.5}$$

By substitution in (12.4) we obtain

$$v_z=-a\frac{\partial j_{\rm ns}}{\partial x}+a\left|\frac{\partial\Gamma}{\partial x}\right|\frac{\Delta(A(m^2))}{\Delta(m)}(m_r+m_l), \tag{12.6}$$

where the second term on the right vanishes in the case of a symmetric profile ($m_l=-m_r$). Now let us calculate the first term:

$$\frac{\partial j_{\rm ns}(x,t)}{\partial x}=\int_{-\infty}^{\infty}du\,\frac{\partial\Gamma(x-u)}{\partial x}\varphi(m(u,t),m'(u,t)). \tag{12.7}$$

Since this term is continuous, we can calculate the derivatives in $x=\xi$. With respect to the angular point, the function $\partial_x\Gamma(x-u)|_{\xi}$ is an odd function of u (positive on the right, negative on the left), and $\varphi(m,m')$ changes sign. So, we can write

$$\frac{\partial j_{\rm ns}(x,t)}{\partial x}=\int_0^{\infty}du\,\left.\frac{\partial\Gamma(x-u)}{\partial x}\right|_0[\varphi(m(u,t),m'(u,t))-\varphi(m(-u,t),m'(-u,t))], \tag{12.8}$$

where the angular point has been located in $\xi=0$. If (11.3) is assumed for the kernel function $\Gamma(u)$ and the quantity in square brackets is considered constant for $u<\varepsilon^{-1}$, we can approximate the previous expression as

$$\frac{\partial j_{\rm ns}(x,t)}{\partial x}=\frac{\varepsilon}{2}[\varphi(m(0^+,t),m'(0^+,t))-\varphi(m(0^-,t),m'(0^-,t))]. \tag{12.9}$$

Finally, the velocity v_z can be rewritten

$$v_z = -\frac{a\varepsilon}{2}\Delta\varphi(m,m') + \frac{a\varepsilon^2}{2}\frac{\Delta(A(m^2))}{\Delta(m)}(m_r + m_l). \quad (12.10)$$

This equation is consistent with the fact that the profiles of Figs. 5(a) and 5(b) are stationary. Indeed $m_r = -m_l$ at all minima and $\varphi = 0$ everywhere on the surface, which implies $v_z = 0$ at all minima.

We conclude that the phenomenological equation (11.2), after having successfully passed a series of tests, seems able to reproduce the results obtained numerically from the Zeno equations of Sec. II. However, its use is limited since we have not been able to write explicitly the function φ. In the following section, it is shown that, nevertheless, a qualitative understanding of the coarsening process may be derived from (11.2).

XIII. MECHANISM OF COARSENING: SMALL MOUNDS

In this section, it will be argued that coarsening, i.e., coalescence of mounds, is a consequence of (11.2), or of Eqs. (12.3) and (12.10) combined with the approximate, local form (10.1) of (11.2), valid away from minima.

Let us assume that most of the mounds are close to the ''universal'' shape defined by $\varphi(m(x),m'(x),m''(x)) = 0$, where the function $\varphi(m,m',m'')$ is defined by (10.3). A qualitative, self-consistent justification of this assumption will be given later. Anyway this assumption is in agreement with simulations.

Suppose now that some mound is smaller than its neighbors (Fig. 11). Because the stationary shape is convex, the slope of this mound at the edges will be weaker than the slope of its neighbors. It follows from this fact and (12.3) that the width of the smaller mound decreases. Therefore the vertical thickness also decreases because the general shape of the mound away from the angular points, as an effect of (10.1) tends to keep close to the ''universal'' shape given by $\varphi(m,m',m'') = 0$. Eventually, the smaller mound disappears and the neighboring ones have grown. At this point, they may be flatter than the universal shape, but further evolution, due to (10.1) and to a vertical motion of the border due to (12.10), brings them again to the universal shape. Thus, coarsening results from smaller mounds being ''eaten'' by bigger ones, a phenomenon which in turn results from Eq. (11.2).

Alternatively, we can say that the stationary configurations found in Secs. V and VIII for $\lambda < \lambda_c^{\sup}$ are stable against height fluctuations, but unstable against width fluctuations. Coarsening is due to this latter property, while the former one keeps the mounds close to the universal form.

Now, in the continuum Zeno model, the universal shape has two vertical asymptotes. Therefore, the above description suggests that coalescence should stop after the mound size has reached a critical value. This value should obviously be identified with the quantity called $\lambda_c^{\sup}$.

The above description of coarsening is in good agreement with our simulations, as will be seen at once. In Fig. 8 we show the temporal evolution of large samples ($\lambda \gg \lambda_c^{\sup}$), for the value $\ell_s/\ell_c = 0.015$. After the very first mounds have appeared, their number decreases in time and the average height increases. More precisely, the largest mounds grow at the expense of the smallest ones. No deep crevace forms till mound width is smaller than the upper critical wavelength.

Regions with positive curvature ($\partial_x m > 0$) are generally present only at the first stages of growth. They may also form just after the death of a mound (see Fig. 8). However, an angular point rapidly arises, in agreement with the fact that in a convex region both terms of the current (6.10) are destabilizing.

Numerical simulations of Zeno equations with random nucleation are also in agreement with the prediction that coarsening stops when the mound radius has reached the value $\lambda_c^{\sup}$. However, when $\lambda > \lambda_c^{\sup}$, the continuous Zeno model ceases to be valid, and the microscopic properties of the material have to be taken into account, for instance, using the prescriptions of Siegert and Plischke.[15] Conjectures concerning this later evolution are presented in the next section.

XIV. MECHANISM OF COARSENING: LARGE MOUNDS

At long times, when mounds are larger than $\lambda_c^{\sup}$, the atomic size should be taken into account. Presumably, it is still possible to define a function $\varphi(m,m',m'') = 0$ and a ''universal'' stationary profile solution of $\varphi(m,m',m'') = 0$. Its asymptotes are no longer vertical, but have a definite slope m^* of order unity as required by Siegert and Plischke.[15] Coalescence is therefore not forbidden even for very big mounds. It is, however, expected to be extremely slow, because when the slope m^* of Siegert and Plischke is reached, the current is zero (this is the definition of m^*) and the profile is stationary. Coarsening is only possible in this later phase because the slope has not exactly the value m^*, but since it is very close to m^*, the coarsening should be very slow as said above.

For a finite system, the final result of coarsening is that a single mound forms, with a slope equal to the characteristic value. However, the evolution of the profile may depend on the microscopic details of the model. Lanczycki and DasSarma[33] have observed the formation of step bunches in this final stage. The reason is possibly that they use a model in which the characteristic slopes of Siegert and Plischke do not exist.

Thus, two phases are expected for the coarsening of a one-dimensional, infinite sample in a model following the Siegert-Plischke scheme: (i) In the first phase, studied in the preceding section, the mound size increases fairly rapidly and the slope remains much smaller than unity. However, if ℓ_s/ℓ_c is very small coarsening proceeds slowly. (ii) In the second phase, the slope is of order unity close to the minima and coarsening proceeds very slowly until the mound size is equal to the sample size. The transition from phase (i) to phase (ii) is characterized by a deepening of crevaces without significant increase of the mound radius.

The previous scheme and formula (12.3) for v_x support the result of simulations by Šmilauer and Vvedensky[16] that coarsening and steepening are competitive: the steeper the mounds are, the slower the coarsening process is.

XV. THREE-DIMENSIONAL CASE

In 2+1 dimensions, it is reasonable to assume the following straightforward generalization of (10.3)

$$\vec{j}(\vec{r},t)=\int \Gamma(\vec{r}-\vec{u})\vec{\varphi}(\vec{m}(\vec{u},t),\vec{\nabla}\vec{m}(\vec{u},t),\nabla^2\vec{m}(\vec{u},t))d^2u, \tag{15.1}$$

where the vector $\vec{m}$ and the tensors $\vec{\nabla}\vec{m}$ and $\nabla^2\vec{m}$ are, respectively, the first, second, and third derivatives of the height z with respect to x and y. The function $\vec{\varphi}$ should have the following form, analogous to (10.3):

$$\vec{\varphi}(\vec{m},\vec{\nabla}\vec{m},\nabla^2\vec{m})=\frac{F\ell_s\ell_c\vec{m}}{2(1+\ell_s|\vec{m}|)(1+\ell_c|\vec{m}|)}-\vec{\nabla}(A(m^2)) +K\theta(|\vec{m}|,|\vec{\nabla}\vec{m}|)\nabla^2\vec{m}, \tag{15.2}$$

where the function $\theta(|\vec{m}|,|\vec{\nabla}\vec{m}|)$ has the same properties as before.

The interest of Eqs. (15.1) and (15.2) is to show the nonlocal and nonlinear character of the problem. As in 1+1 dimensions, no local continuous equation can account for the slope discontinuities which are now expected to occur on angular *lines* rather than angular points. However, Eqs. (15.1) and (15.2) are much less tractable yet than their equivalent in 1+1 dimensions. For instance, even if equations similar to (12.3) and (12.10) can be written in 2+1 dimensions, they will not be as predictive as in 1+1. The possibility of dislocations and disclinations in the network of mounds gives a higher complexity to the (2+1)-dimensional case.

XVI. CONCLUSIONS

We have investigated a (1+1)-dimensional model of a high-symmetry growing surface. Surface grows by a deterministic movement of the steps and by a random nucleation of new terraces.

The stochastic character of the nucleation process is of great importance during the first stages of the growth and it makes a mound structure arise only after a time $t^*\sim 1/\ell_s^2$, with a wavelength $\lambda_c^{\inf}\sim 1/\sqrt{\ell_s}$. This means that possible defects of the surface are healed during the growth if their size is smaller than $\lambda_c^{\inf}$ [see, for example, the case of GaAs (Ref. 7)].

During this first period, random nucleation is well accounted for a linear term $(K\partial^2 m/\partial x^2)$ in the current j, which must be added to the Schwoebel current j_s.

At later times mounds form and they are separated by angular points. The existence of these structures is due to a current j_c, which depends on the curvature of the surface and in regions of negative curvature $(\partial_x m<0)$ may compensate j_s.

After mounds have formed, a coarsening process starts, because a periodic profile is not stable with respect to lateral fluctuations. Coarsening is mainly a deterministic process, driven by an asymmetry between the left and right slopes at the angular point. At increasing times, the coarsening process becomes slower, because of the steepening of the mounds. When λ is larger than $\lambda_c^{\sup}\sim 1/\ell_s$, our model predicts that coarsening stops and grooves become deeper and deeper.

We can compare our findings with the results of other models. Generally speaking, three different scenarios can be singled out: in the first one (Siegert and Plischke,[15] Šmilauer and Vvedensky,[16] Amar and Family[17]) mounds attain a self-similar structure and the maximum slope keeps constant. Anyway, the limiting slopes differ a lot and may be due to crystal structure effects,[15] to kinetic effects,[16] or both.[17] A simple explanation of the kinetic effects is not available at the moment.

In the second scenario (Hunt *et al.*[19]) mounds become steeper and steeper, with no limiting value for λ. Finally, in the third one (proposed in the present paper) there is no slope selection either, but an upper critical wavelength does exist. Both the second and third scenarios should have a crossover to the first one for $m\approx 1/a$, if the discrete nature of the lattice would be correctly taken into account.

It is interesting to wonder whether this scenario survives when thermal detachment of atoms from steps is allowed. We think it does, if the probability of detachment is sufficiently small, i.e., if the temperature is sufficiently low. In fact, in absence of detachment, for $\lambda>\lambda_c^{\sup}$, the height of the mounds increases linearly with time, at a positive velocity v_h which depends on ℓ_s. So, if the rate of detachment is smaller than v_h, the upper critical wavelength still exists, while if the rate is larger than v_h, $\lambda_c^{\sup}$ is probably infinite and the second scenario becomes pertinent.

Our model is peculiar also in another respect: we do not obtain a powerlike behavior for the coarsening law, $\lambda(t)\sim t^n$. Usually, such a law would only be expected in the ''self-similar'' regime (first scenario). Anyway, both in experiments and in simulations, it is observed even if the slope does not stay constant. In this case, the origin of such powerlike behavior is not clear.

ACKNOWLEDGMENTS

I. Elkinani is gratefully acknowledged for the permission to make use of its routines and for his help during the first stages of this work. We also thank P. Šmilauer and L.M. Sander for illuminating discussions. P. Politi acknowledges financial support from the EEC program Human Capital and Mobility, under Contract No. ERBCHBICT941629.

APPENDIX A: NUMERICAL CALCULATIONS ON SMALL SAMPLES

The numerical calculations of the following two sections are carried out by solving the Zeno coupled equations [(2.5)–(2.9)] for the step motion. Details are given in Ref. 18. Two possible models can be used: a ''completely continuous'' model, where there is no room for the interatomic distance a and a ''quasicontinuous'' model, where the Schwoebel barrier is turned off for terraces smaller than a. This does not prevent small terraces, but anyway it limits the depth of the crevaces when they form. If not differently specified, we will always use the finite value $a=0.005\ell_c$. Also, the value of the nucleation length ℓ_c is everywhere taken as 1.

1. Deterministic nucleation

Let us start by summarizing the temporal evolution of small samples with a single pyramid *per* period (see Fig. 2). Each pyramid is characterized by its width L (which equals

the period λ in this case) and by its height $h(0)$ at $t=0$; another important quantity is the starting terrace length $\ell=L/2h(0)$. The period L is obviously a constant, while h changes with time. The Schwoebel length is fixed at the value $\ell_s/\ell_c=0.015$. The main results are the following.

(i) A threshold value $\lambda_c^{\rm sup}$ *does* exist for the rising of the instability; if $L>\lambda_c^{\rm sup}$, and $h(0)$ is not too small, a crevace appears and its depth increases with time.

(ii) For $L<\lambda_c^{\rm sup}$ we have stationary configurations. If $h(0)$ is sufficiently high, so that nucleation takes place only on top terraces [$h(0)>L/2\ell_c\equiv h_{\rm min}$], the stationary configuration is a pyramid whose height h_∞ depends on L: the steady value h_∞ grows with L, but it does not go to infinity when L goes to $(\lambda_c^{\rm sup})^-$. Rather, for $\ell_s=0.015$ we observe that $\lim_{L\to(\lambda_c^{\rm sup})^-}h_\infty=15$. It is important to stress that this result does not depend on the value of the lattice constant a, the only difference being a slightly different value of $\lambda_c^{\rm sup}$. For example, $\lambda_c^{\rm sup}=9.397$–$9.398$ for $a=5\times10^{-3}$ and $\lambda_c^{\rm sup}=9.391$–$9.392$ for $a=0$. However, in both cases, the largest value of h_∞ is 15.

(iii) If $h(0)$ is slightly larger than $h_{\rm min}$, h increases monotonically with time, until $h=h_\infty$. If $h(0)$ is higher, then $h(t)$ increases almost linearly with time, until a value t_L at which the crevace is healed, *via* step bunching. The value t_L increases with $h(0)$ and with L. If $h(0)$ is fixed, t_L seems to go to infinity when $L\to(\lambda_c^{\rm sup})^-$.

(iv) If $h(0)$ is sufficiently small [$h(0)<h_{\rm min}$], nucleation takes place also on vicinal and bottom terraces, and trivial steady configurations are found.

Similarly, we can fix the width L by varying the Schwoebel length ℓ_s. In both the cases we conclude that a finite value of ℓ_s is required to create an instability in a finite sample. When ℓ_s goes to zero, $\lambda_c^{\rm sup}(\ell_s)$ goes to infinity.

2. Random nucleation

In the case of RN as well, we obtain pyramid-like stationary configurations, similarly to the DN case (see Fig. 6). Anyway, the critical length λ_c^{sup} is much larger in the random case: random nucleation stabilizes the growth against the Schwoebel effect.

The effect of randomness on the growth is twofold: (i) it makes stochastic the nucleation on top terraces (where most of the nucleations takes place) and (ii) it implies a finite probability of nucleation on vicinal terraces. Let us recall that in the deterministic model, the nucleation of a new terrace takes place only when $\ell>\ell_c$. For a vicinal terrace, if this condition is not fulfilled at $t=0$, it generally remains unfulfilled also at later times. The second effect (nucleation on vicinal terraces) is seen to be stabilizing, since it reduces the Schwoebel current.

Since the probability $P(\ell)$ of nucleation is very weak for $\ell<\ell_c$ and stationary profiles seem to be characterized by few events of nucleation on vicinal terraces (Fig. 6), we could conclude that the second effect is negligible, but it is not so. For example, let us consider the evolution of a ''steady'' configuration, obtained *via* random nucleation. This means that a further evolution with RN does not modify the main characteristic of the surface profile, i.e., the interface width. But, if we consider the artificial evolution determined by RN on top terraces and DN elsewhere, we find that the surface undergoes an instability, so random nucleation on vicinal terraces is an important source of stabilization.

Random nucleation not only increases $\lambda_c^{\rm sup}$, but it also changes the shape of the stationary configurations, which are characterized by a large ''flat'' region on the top of the mounds. It may be reasonable to identify the width of this region on the lower critical wavelength, $\lambda_c^{\rm inf}$.

APPENDIX B: STUDY OF Eq. (3.3)

In this Appendix we want to justify formula (3.3). This formula, which neglects asymmetry effects [second term in Eq. (10.3)] and uses a linear form, for the term containing $\partial^2 m/\partial x^2$, allows for an analytical determination of stationary configurations. We will do that, by following the method of Hunt *et al.*[19]

We have said in the main text that the first term, the Schwoebel current j_s, results from an interpolation of (3.1), valid at high slopes, and (1.3) which is expected to be correct for $|m|\ll\ell_c^{-1}$. Let us start by justifying expression (1.3).

When $\ell>\ell_c$ a new terrace nucleates on it, so there are no terraces larger than ℓ_c. We shall suppose in this case that $\ell\simeq\ell_c$, and the current will be calculated as an average on all the terraces. We must however distinguish among top or bottom terraces (which do not contribute to the current) and vicinal ones, which may be of two types, according to the sign of the current.

If n_+,n_-,n_0 are the number of terraces in each class (respectively, vicinal up, vicinal down and top or bottom), subdivided according to the current, we will have [see (3.1)]

$$j_s=\frac{F\ell_s}{2(1+\ell_s/\ell_c)}\left(\frac{n_+-n_-}{n_++n_-+n_0}\right) \tag{B1}$$

because each vicinal terrace contributes with a quantity $j_\pm=\pm F\ell_s/[2(1+\ell_s/\ell_c)]$.

We are interested in the dependence of j_s on the average slope

$$m=\frac{1}{\ell_c}\left(\frac{n_+-n_-}{n_++n_-+n_0}\right) \tag{B2}$$

so that

$$j_s=\frac{F\ell_s\ell_c}{2(1+\ell_s/\ell_c)}m. \tag{B3}$$

It is noteworthy that the two limiting expressions (B3) and (3.1) coincide for $|m|=1/\ell_c$.

Now, let us study the stationary solutions of (3.3), by following the method of Hunt *et al.*[19] Stationary solutions correspond to a vanishing current, that is to say

$$K\frac{d^2m}{dx^2}=-j_s(m). \tag{B4}$$

Formally, this is the equation of motion of a particle of mass K, whose (one-dimensional) spatial coordinate is m and x corresponds to the time. The potential is

$$V(m)=\int dm j_s(m). \tag{B5}$$

Substituting the first term of (3.3) in (B5), it is easily found, in the limit $\ell_c \gg \ell_s$ and up to a constant, that

$$V(m)=\frac{F\ell_s}{2}\left[\frac{1}{\ell_s}\ln(1+|m|\ell_s)-\frac{1}{\ell_c}\ln(1+|m|\ell_c)\right]. \tag{B6}$$

The absence of slope selection during the coarsening process can be directly inferred from (B6), since $V(m)$ is a single well potential and no upper limit for m exists.

The equivalence with the particle model leads us to define the ''energy''

$$\frac{1}{2}K\left(\frac{dm}{dx}\right)^2+V(m)=V(M), \tag{B7}$$

where M is the maximal slope of the stationary configuration, at fixed wavelength. The wavelength λ is

$$\lambda=4\int_0^M \frac{dm}{(dm/dx)}=4\sqrt{\frac{K}{2}}\int_0^M \frac{dm}{\sqrt{V(M)-V(m)}}. \tag{B8}$$

At small m we can expand $V(m)$

$$\begin{aligned} V(m) &\simeq \frac{F\ell_s}{2}\left\{\frac{1}{\ell_s}\left[m\ell_s-\frac{1}{2}(m\ell_s)^2\right]\right. \\ &\quad \left.-\frac{1}{\ell_c}\left[m\ell_c-\frac{1}{2}(m\ell_c)^2\right]\right\} \\ &\simeq \frac{F}{4}\ell_s\ell_c m^2 \end{aligned} \tag{B9}$$

and obtain for λ

$$\begin{aligned} \lambda(M\to 0) &\simeq 4\sqrt{\frac{K}{2}}\sqrt{\frac{4}{F\ell_s\ell_c}}\int_0^M \frac{dm}{\sqrt{M^2-m^2}} \\ &\simeq 2\pi\sqrt{\frac{2K}{F\ell_s\ell_c}}. \end{aligned} \tag{B10}$$

This coincides with the expression (3.6) for the lower critical wavelength $\lambda_c^{\inf}$.

In the opposite limit ($M\to\infty$), the period λ is given by

$$\begin{aligned} \lambda &= 4M\sqrt{\frac{K}{F\ell_s}}\int_0^1 \frac{dy}{\sqrt{\ln[(y+1/M\ell_s)^{-1/\ell_s}(y+1/M\ell_c)^{1/\ell_c}]}} \\ &\simeq 4M\sqrt{\frac{K}{F}}\int_0^1 \frac{dy}{\sqrt{\ln(1/y)}} \end{aligned} \tag{B11}$$

and the height of the stationary configuration by

$$\delta z=\int_0^M dm\,\frac{m}{dm/dx}\simeq M^2\sqrt{\frac{K}{F}}\int_0^1 dy\,\frac{y}{\sqrt{\ln(1/y)}}. \tag{B12}$$

As expected, M goes to infinity with λ. The result (B11) could be qualitatively obtained by observing that in the limit of high slopes, condition (B4) writes

$$K\frac{M}{\lambda^2}\approx F\frac{1}{M} \tag{B13}$$

or $M\approx\sqrt{F/K}\lambda$, as given by (B11).

[1] G. Ehrlich and F.G. Hudda, J. Chem. Phys. **44**, 1039 (1966).

[2] R.L. Schwoebel and E.J. Shipsey, J. Appl. Phys. **37**, 3682 (1966); R.L. Schwoebel, *ibid.* **40**, 614 (1969).

[3] J. Villain, J. Phys. (France) I **1**, 19 (1991).

[4] J. Villain and A. Pimpinelli, *Physique de la Croissance Cristalline* (Eyrolles-Alea-Saclay, Paris, 1994) and English version (Cambridge University Press, Cambridge, England, in press).

[5] D.J. Eaglesham, H.J. Gossmann, and M. Cerullo, Phys. Rev. Lett. **65**, 1223 (1990).

[6] J.E. Van Nostrand, S. Jay Chey, M.-A. Hasan, D.G. Cahill, and J.E. Green, Phys. Rev. Lett. **74**, 1127 (1995).

[7] C. Orme, M.D. Johnson, J.L. Sudijono, K.T. Leung, and B.G. Orr, Appl. Phys. Lett. **64**, 860 (1994).

[8] M.D. Johnson, C. Orme, A.W. Hunt, D. Graff, J. Sudijono, L.M. Sander, and B.G. Orr, Phys. Rev. Lett. **72**, 116 (1994).

[9] H.J. Ernst, F. Fabre, R. Folkerts, and J. Lapujoulade, Phys. Rev. Lett. **72**, 112 (1994); J. Vac. Sci. Technol. A **12**, 1809 (1994).

[10] M. Albrecht, H. Fritzsche, and U. Gradmann, Surf. Sci. **294**, 1 (1993).

[11] K. Thürmer, R. Koch, M. Weber, and K.H. Rieder, Phys. Rev. Lett. **75**, 1767 (1995).

[12] J.A. Stroscio, D.T. Pierce, M.D. Stiles, A. Zangwill, and L.M. Sander, Phys. Rev. Lett. **75**, 4246 (1995).

[13] D.J. Eaglesham and G.H. Gilmer, in *Surface Disordering: Growth, Roughening and Phase Transitions*, edited by R. Jullien, J. Kertèsz, P. Meakin, and D.E. Wolf (Nova Science, New York, 1993).

[14] Z. Zhang, J. Detch, and H. Metiu, Phys. Rev. B **48**, 4972 (1993).

[15] M. Siegert and M. Plischke, Phys. Rev. Lett. **73**, 1517 (1994).

[16] P. Šmilauer and D.D. Vvedensky, Phys. Rev. B **52**, 14 263 (1995).

[17] J. Amar and F. Family, Phys. Rev. B (to be published).

[18] I. Elkinani and J. Villain, Solid State Commun. **87**, 105 (1993); J. Phys. (France) I **1**, 1991 (1994). These authors oversimplified the expression (2.2) of ℓ_s as a function of D' by omitting the -1 as would be correct for a strong Schwoebel effect. This is generally not justified since the case of interest is that of a weak Schwoebel effect, when ℓ_s/ℓ_c is very small, so that the growing surface remains smooth for a long time. Since D' plays no part in the remainder of their articles, this mistake has no consequence.

[19] A.W. Hunt, C. Orme, Williams, B.G. Orr, and L.M. Sander, Europhys. Lett. **27**, 611 (1994).

[20] J.A. Stroscio and D.T. Pierce, Phys. Rev. B **49**, 8522 (1994).

[21] J. Krug and M. Schimschak, J. Phys. (France) I **5**, 1065 (1995).

[22] Sometimes (see, for example, Ref. 21), a term proportional to ρ^2 is added to the right-hand side of (2.4), to take into account nucleation events. This is generally done on a vicinal surface, so as to generalize the Burton, Cabrera, and Frank theory (Ref. 23). In our case, we study a high-symmetry surface, so that a distinction between underlying steps—which give the boundary conditions for (2.4)—and the steps of newly nucleated terraces, is not possible. Also, such a correction to (2.4) would not allow to study the stochasticity of nucleation [see Eq. (2.10)].

[23] W.K. Burton, N. Cabrera, and F. Frank, Philos. Trans. R. Soc. London **243**, 299 (1951).

[24] G. Zinnsmeister, Thin Solid Films **2**, 497 (1968); *ibid.* **7**, 51 (1971).

[25] S. Stoyanov and D. Kashchiev, in *Current Topics in Material Science*, edited by E. Kaldis (North-Holland, Amsterdam, 1981), Vol. 7, p. 69.

[26] J.A. Venables, G.D. Spiller, and M. Hanbücken, Rep. Prog. Phys. **47**, 399 (1984).

[27] J. Krug, Habilitation thesis, Juelich, Duesseldorf, 1995. See also Ref. 16 for a discussion of formula (3.8).

[28] T. Sun, H. Guo, and M. Grant, Phys. Rev. A **40**, 6763 (1989).

[29] D.E. Wolf and J. Villain, Europhys. Lett. **13**, 389 (1990).

[30] S. Das Sarma and P. Tamborenea, Phys. Rev Lett. **66**, 325 (1991).

[31] P. Politi and J. Villain, *Proceedings of the Mato Conference on Surface Diffusion (Rhodes, Greece)* (Plenum, New York, in press).

[32] M. Kardar, G. Parisi, and Y.-C. Zhang, Phys. Rev. Lett. **56**, 889 (1986).

[33] C.J. Lanczycki and S. Das Sarma, Phys. Rev. Lett. **76**, 780 (1996).